Int. J. Electrochem. Sci., 15 **(2020)** 1881 – 1892, doi: 10.20964/2020.03.63

International Journal of
ELECTROCHEMICAL
SCIENCE
www.electrochemsci.org

Effect of Sintering Conditions on Electrochemical Properties of $LiNi_{0.8}Co_{0.1}Mn_{0.1}O_2$ as Cathode Material

Jing Li[1], *Maolin Zhang*[1,*], *Dongyan Zhang*[1], *Yangxi Yan*[1], *Zhimin Li*[1], *Zhiqiang Nie*[2,*]

[1] School of Advanced Materials and Nanotechnology, Xidian University, Xi'an, 710071, China
[2] Xi'an Institute of Optics and Precision Mechanics, Chinese Academy of Sciences, Xi'an, 710119, China
[*]E-mail: mlzhang@xidian.edu.cn, niezq@opt.ac.cn

Received: 9 November 2019 / *Accepted:* 7 January 2020 / *Published:* 10 February 2020

Many works of literature have reported the drastic effects of synthesis methods on the electrochemical performances of Ni-rich cathode materials $LiNi_{0.8}Co_{0.1}Mn_{0.1}O_2$ (NCM811). In this research, a two-step sol-gel method was successfully employed to synthesize pure NCM811 and the process of preparation is discussed in detail. The electrochemical properties depending on the structures and morphologies were verified by the multichannel galvanostatic system, EIS, XRD, and SEM. The results clarified that when the precursor was sintered at 750 °C for 15 h, the sample exhibited dominant electrochemical properties with initial discharge capacities of 230.8 and 176.3 mAh/g at 0.1 and 1 C, respectively. Moreover, the capacity retention rate is as high as 79% after 100 cycles at 1 C. These excellent electrochemical properties were considered to be arriving from the well-developed layered structure and low charge transfer resistance.

Keywords: Cathode materials; $LiNi_{0.8}Co_{0.1}Mn_{0.1}O_2$ (NCM811); Electrochemical properties; Sol-gel method

1. INTRODUCTION

Lithium-ion batteries (LIBs) which possess the qualities of dominant specific capacity, environmental friendliness, excellent cycle performance and low-cost, have been comprehensively applied to electric vehicles, digital products and so on [1-2]. Cathode material as a dynamic component of LIBs has become a vital factor that regulates its utilization [3]. Recently, a Ni-rich layered cathode material $LiNi_{0.8}Co_{0.1}Mn_{0.1}O_2$ (NCM811) having the advantages of excellent theoretical capacity [4], raised up reversible capacity [5] and cost-effectiveness [6] has been considered as the most promising candidate.

However, the flaws of rapid capacity fading and poor rate capability pose enormous hurdles in the application of NCM811[7]. There are still numerous problems that exist in the production of Ni-rich layered cathode materials. Li vacancy (V_{Li}) as well as O vacancy (V_O) tend to form during the high-temperature synthesis procedure credited to the volatilization of Li and oxygen during escape. Besides, a high-energy barrier essentially strides across, when Ni^{2+} converts to Ni^{3+}. The size, morphology of the particles and the crystallinity of the materials, which are determined by the synthesis methods, do drastically influence the performance of the active constituents. As a result, a proper method that can alleviate these problems should be explored.

According to the literature, Ni-rich layered-cathode materials can be produced by various methodologies such as co-precipitation method [8-11], solid-state method [12-13], combustion synthesis [14-15], sol-gel method [16-20], spray pyrolysis [21-22], hydrothermal method [23], and so on. Among these, the co-precipitation method is one of the most commonly used methods till date. Ni, Co, Mn atoms can be distributed homogeneously at a molecular level by utilizing this method [10]. A spherical precursor owning uniform size and high vibration density which will lead to superior electrochemical properties of the as-prepared cathode materials, can be synthesized by this method [8]. The effects of starting materials, pH, temperature, mixing time etc., on the high tap-density and uniform-sized distribution of precursors have been fully explored [24]. Yet, defects such as long reaction times, complex operational methods and high costs are still the main problems that impede the widespread application of the co-precipitation method [25].

The solid-state method is the most often utilized synthetic process in industrial manufacturing owing to its cost-efficiency, process simplicity and accurate stoichiometric ratios. In the standard method of this approach, the transition metal (Ni, Co, Mn) and Li nitrates, acetates, oxides etc., are utilized as starting materials and uniformly blended by ball-milling [26]. Then the mixture is calcined at an appropriate temperature for many hours until the cathode material is successfully prepared. Xia has discussed in detail, the effects of sintering temperature and time on the performance of NCM622 [27]. In our earlier study [28], the effect of particle size on the electrochemical performances of the NCM811 cathode material was precisely researched. Yet, the starting materials could not be mixed uniformly by using this method which led to uneven particle sizes as well as poorer electrochemical properties of cathode materials.

Wook Ahn [15] established that NCM622 can be successfully synthesized by employing the combustion synthesis method. The as-prepared NCM622 exhibited an initial discharge capacity of 170 mAh/g (at 20 mA/g) and the capacity retention of 98.2% after 30 cycles. Then, spray pyrolysis method having the advantages of high effectivity and short synthetic process, was employed to prepare NCM811 by Li [21]. The specific discharge capacity was so dominant that it can reach 173 mAh/g after 100 cycles at 1C rate. Moreover, a single-crystal and splendid-performance cathode material (153.6 mAh/g at 10 C) was obtained via the hydrothermal method developed by Wang [23]. Yet, the aforementioned approaches cannot be extensively applied due to weaknesses such as inferior security, heterogeneity of the prepared materials and long reaction periods. Consequently, a relatively versatile, simple and convenient method should be explored to produce materials with dominant electrochemical properties.

The sol-gel method is another frequently applied synthetic procedure to prepare Ni-rich layered cathode materials. Cathode materials with homogeneous distribution of elements as well as submicron-sized particles, leading to exceptional electrochemical characters can be prepared by this process [19]. Moreover, this technique is more convenient and simpler than the co-precipitation method [18]. Lu synthesized NCM811 via this method and found superior electrochemical properties owing to the lower Li/Ni disorder and larger specific surface area compared to the co-precipitation method [17]. Nonetheless, the experimental details were seldom discussed. Hence, to investigate the intricacies of this system, a two-step sol-gel method was utilized to synthesize NCM811 cathode materials and the synthetic process was discussed in detail in this work. The structures and morphologies of the as-prepared NCM811 were characterized by XRD and SEM. In addition, a multichannel galvanostatic system together with EIS was applied to further explore the electrochemical properties.

2. EXPERIMENTAL

2.1 Preparation

NCM811 cathode powders were prepared in two steps. Initially, the $Ni_{0.8}Co_{0.1}Mn_{0.1}(OH)_2$ precursor was synthesized via the sol-gel method by using $Ni(NO_3)_2•6H_2O$, $Co(NO_3)_2•6H_2O$, $Mn(NO_3)_2•4H_2O$ and citric acid (CA) as starting reagents. These reagents were dissolved in distilled water in a molar ratio of Ni:Co:Mn: CA = 8:1:1:10 and were vigorously stirred for 4 h to acquire a well-mixed solution. Then, this mixture was heated and agitated at 60 °C for 4 h followed by immediate drying by oven-heating until the gel was obtained.

Next, $Li(OH)•H_2O$ as the lithium source, was well-blended through grinding with the gel obtained in the first step. After being preheated at 400 °C for 3 h, the blended powders were then sintered at different temperatures and sintering preservation times, until NCM811 cathode powders were obtained, as shown in Table 1.

Table 1. Samples of the obtained NCM811

Sample	NCM-700	NCM-750	NCM-800	NCM-850	NCM-12	NCM-18
Temperature	700 °C	750 °C	800 °C	850 °C	750 °C	750 °C
Time	15 h	15 h	15 h	15 h	12 h	18 h

Coin cells (CR-2016) that would be employed for exploring the electrochemical properties, were assembled as literature reported [29]. The as-obtained NCM811 powder, carbon black, PVDF and NMP were applied as the active material, a conductive additive, binder, and solvent respectively. After being well-mixed together by ball-milling for 4 h, the slurry was produced and then was coated on an Al foil to form positive electrodes. In this work, Li metal was used as the anode, microporous

polypropylene membrane (Celgard 2400) was utilized as the separator and $LiPF_6$ was employed as the electrolyte.

3. RESULTS AND DISCUSSION

3.1 Effect of sintering temperature

3.1.1 Structure and morphology

XRD patterns of NCM811 samples synthesized at different temperatures are shown in Figure 1. It is clear that there existed some impurity phase when sintering was done at 700 °C. When the sintering temperature reached 750 °C, no obvious impurity phase could be observed, signifying that for the production of pure-phase NCM811, the starting materials need to be sintered above 750 °C. As we can see, the diffraction peaks of the samples agree to the hexagonal α-$NaFeO_2$ structure of R-3m space group (PDF, No: 74-0919) [4]. Moreover, the obvious split of (006)/(102) and (108)/(110) peaks, that illustrate the noticeable layered structure, can be observed in the samples NCM-750 and NCM-800, as shown in Figure 1(B) [29]. Conversely, the splitting of the peaks at (006)/(102) and (108)/(110) for NCM-700 is implicit, indicating the terrible nature of the developed layered structure, which is well consistent with the result reported by Wang [30]. Furthermore, the c/a value is 4.9307, 4.9468, 4.9467 and 4.9405 for sample NCM-700, NCM-750, NCM-800, and NCM-850, respectively. In other words, the sample NCM-750 synthesized at 750 °C displays the highest c/a value, conforming to a well-formed layered structure [26].

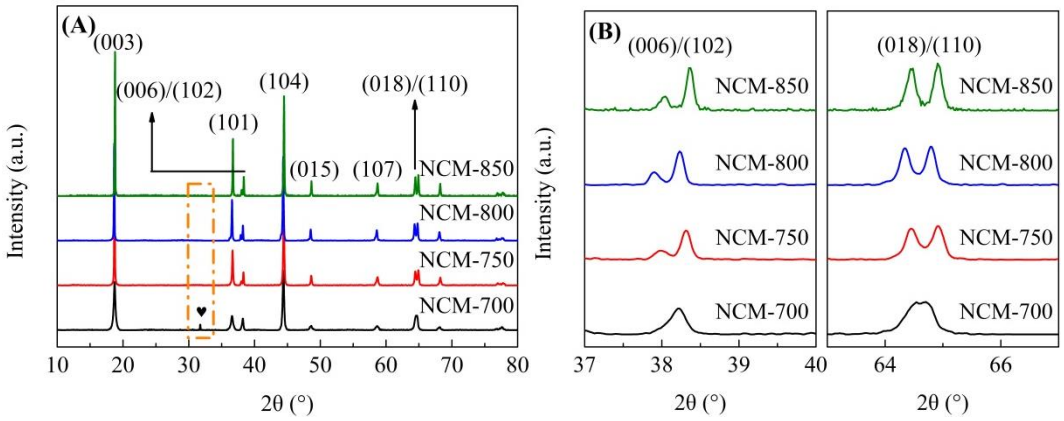

Figure 1. XRD patterns of NCM811 powders prepared at different temperatures.

Figure 2 displays the SEM images of NCM811 prepared at different temperatures. The particle sizes increase with the increase in sintering temperature. This phenomenon is typical of the morphological features of particles synthesized by the sol-gel method [17]. When the sintering temperature is 700 °C there are numerous tiny particles attached to the large particles, indicative of the temperature not being high enough for their growth. As is shown in the SEM images, particles with

diameters in the range of 300-500 nm get distributed homogeneously under the condition of 750 °C which later leads to dominant and stable electrochemical performances. With further raising of sintering temperature, the particles grow larger with uneven particle-size distribution, indicative of the rapid degradation of resultant electrochemical performances.

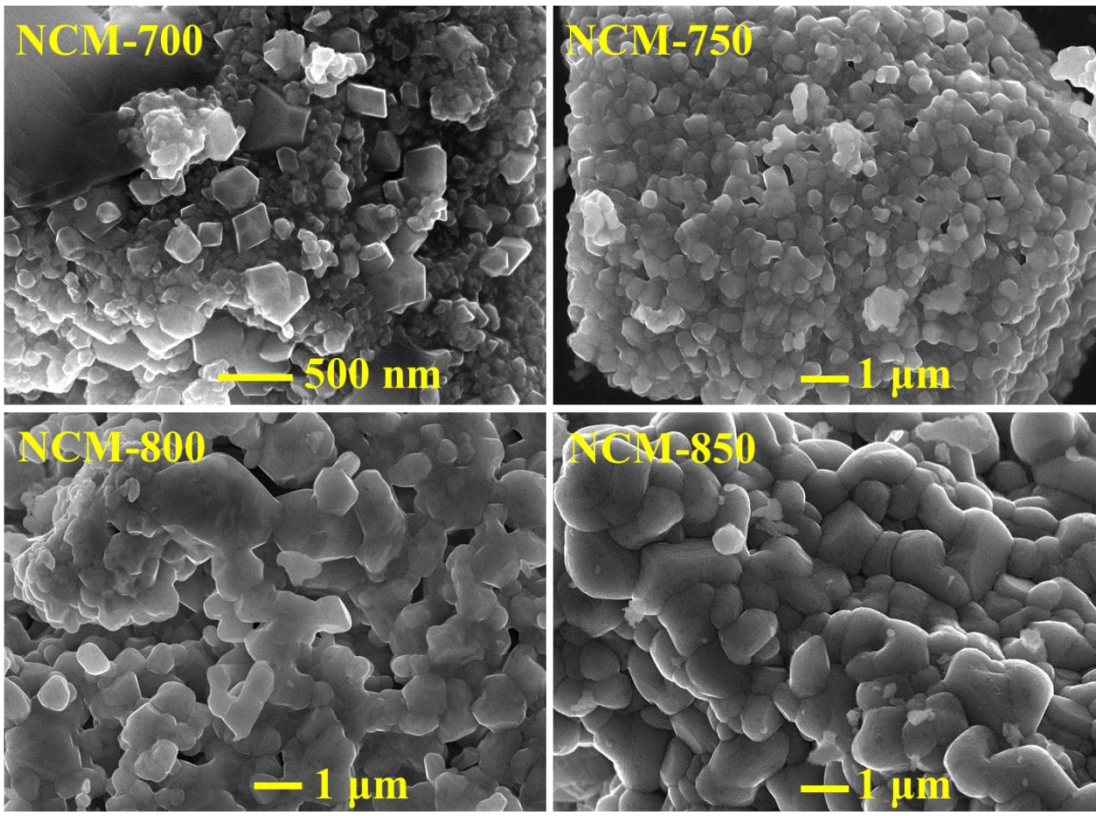

Figure 2. SEM images of NCM811 powders prepared at different temperatures.

3.1.2 Electrochemical Performances

The preliminary charge/discharge properties of various cathode materials were tested at 0.1 C within a range of 2.7-4.3 V and are presented in Figure 3 (A). With sintering temperature being raised, the preliminary charge/discharge capacity initially increases and subsequently decreases. The sample NCM-750 shows the highest discharge value of 230.8 mAh/g at 0.1 C, while the discharge capacity of the samples NCM-700, NCM-800 and NCM-850 were 153.4, 215.6 and 202.3 mAh/g, respectively. In addition, the cycle performance was verified by the galvanostatic system at a rate of 1 C and the results are presented in Figure 3 (B). Likewise, the sample NCM-750 displays a superior discharge capacity of 176.3 mAh/g at 1 C and more than 79% of its capacity was retained after 100 cycles. Nonetheless, the capacity retention rate is only 67% and 68% respectively, for the samples NCM-700 and NCM-850 after 100 cycles. NCM-700 represents inferior first-discharge capacity and cycling performance attributed to the impure phase which affects its structural stability, as shown in Figure 1(A). Besides, these results are considered attributed to the high crystallinity of the cathode powders in addition to the homogeneous distribution of the particle sizes. As reported in Yang's work [31], a uniform distribution

of particle size can help to avoid volume effect as well as increase the tap density. The difference in stress variation during the lithiation/delithiation process of Li^+ may be weakened owing to the homogeneous nature of particle sizes, which will lead to excellent cycling performance. This result is corresponding to the influence of morphology on the electrochemical performance in Hua's work [32].

In addition, the rate capabilities of the samples were tested at 0.1~5 C as presented in Figure 3 (C). The sample NCM-750 displays the highest rate capability and its discharge capacity is 200.2, 195.3, 175.0, 157.5, 139.8, and 108.3 mAh/g when tested at various rates (0.1 C to 5 C). The spectacularly high capacity at 5 C rate is primarily due to the moderate particle size and a high diffusion coefficient of Li^+ [33-34]. Wang [33] has confirmed that cathode material showed the highest discharge capacity of 159.7 mAh/g at 5 C rate based on the highest $D_{Li}{}^+$. It is worth mentioning that the discharge capacity is as high as 201.9 mAh/g after the rate cycle period, signifying that the crystal structure of the cathode material is hard to destroy during the lithiation/delithiation process even at a high rate.

EIS measurements were applied to further establish the electrochemical properties of prepared cathode materials and the results are presented in Figure 3 (D) and (E). Apparently, the curves that were collected after 1st and 100th cycles, contain two semicircles and a straight line [10]. The fitted EIS parameters are listed in Table 2. Generally, R_s, R_{sf} and R_{ct} represent the resistance of Li^+ transporting in the electrolyte, resistance at the solid electrolyte interface (SEI) and the charge transfer resistance [28]. R_{ct} is a significant parameter that seriously influences the electrochemical performance of the cathode material. As reported by Fan [35], R_{ct} value of various samples exhibited substantial difference after cycles leading to a diversity in performance. The initial R_{ct} values of NCM-700, NCM-750, NCM-800, and NCM-850 after the first cycle is 952.4, 179.9, 199 and 247.7 Ω respectively which further escalates to 2476, 404.2, 410.5 and 643.4 Ω when cycling is carried out for 100 times. The R_{ct} of all the samples increases after 100 cycles mainly because of the thickening of the solid electrolyte interface [36]. Even though the R_{ct} of NCM-750 increases from 179.9 Ω to 404.2 Ω after 100 cycles, it still displays a minimum value among all the samples. It has been demonstrated that the small resistance is a result of low polarization which will lead to superior electrochemical properties [37].

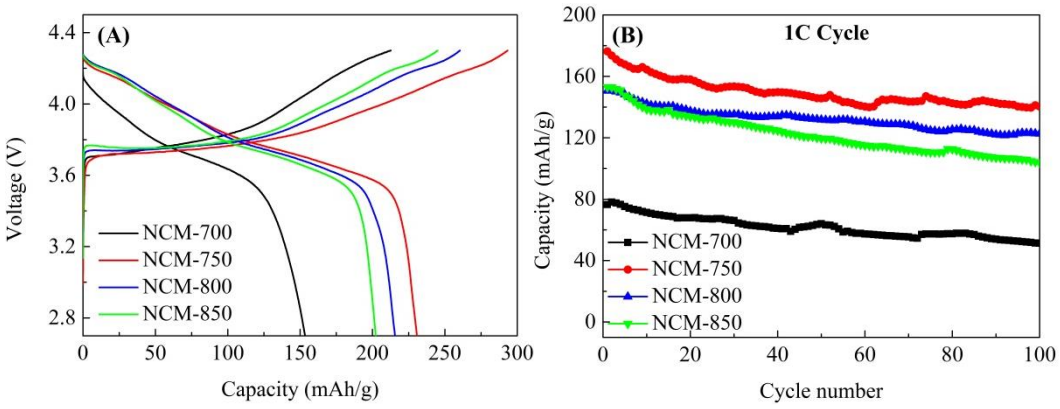

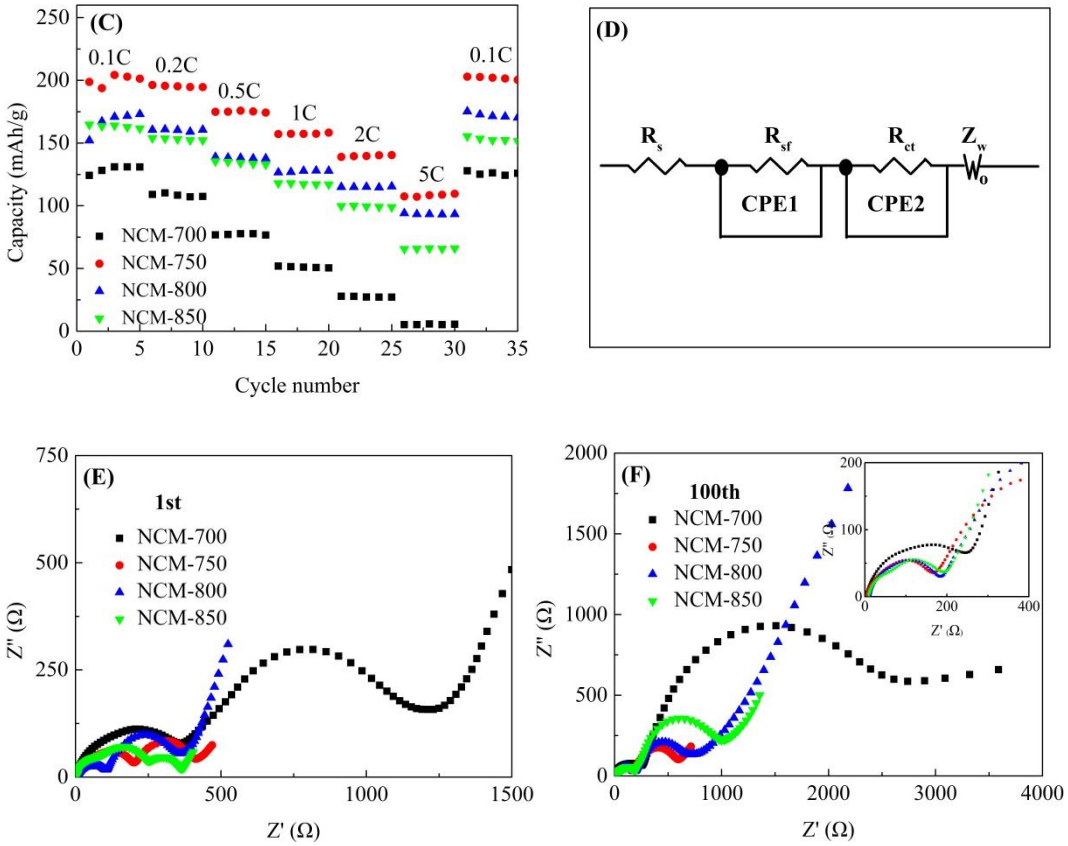

Figure 3. Electrochemical properties of NCM811 cathode materials prepared at different temperatures. (A) Initial charge/discharge properties at 0.1 C, (B) Cycling performance at 1 C, (C) Rate capabilities, (D) Equivalent resistance diagram, (E) EIS curves for the initial cycle, (F) EIS curves after 100 cycling.

Table 2. Fitted parameters obtained from EIS shown in Figure 3 (E) and (F).

Sample	At the 1st cycle			At the 100th cycle		
	$R_s(\Omega)$	$R_{sf}(\Omega)$	$R_{ct}(\Omega)$	$R_s(\Omega)$	$R_{sf}(\Omega)$	$R_{ct}(\Omega)$
NCM-700	2.829	314.7	952.4	6.6436	200.7	2476
NCM-750	1.901	206.6	179.9	2.665	173.5	404.2
NCM-800	2.121	99.37	199	9.961	169.6	410.5
NCM-850	2.264	42.95	247.7	6.914	188.7	643.4

3.2 Effect of sintering time

3.2.1 Structure and morphology

Figure 4 shows XRD patterns of the samples sintered at 750 °C for different times. No impure phases can be observed at this juncture. Moreover, all the samples retain distinct (006)/(102) and

(108)/(110) splitting peaks demonstrating that the prepared powders have ordered layer structures. As a result, it can be inferred that sintering time between 2-18 hours, has no obvious effect on the crystal structure. On the other hand, the c/a value of NCM-12, NCM-750 and NCM-18 is 4.9441, 4.9468 and 4.9444, respectively, indicating NCM-750 exhibits best-layered structure. Meanwhile, SEM was utilized to analyze the morphologies of the obtained powders that underwent preservation at different times. The particles of all the samples are spheroids having the diameters in the range of 300-500 nm which confirms that the sintering time has little influence on the morphologies of the cathode material. Similar results have been reported by Xia [27].

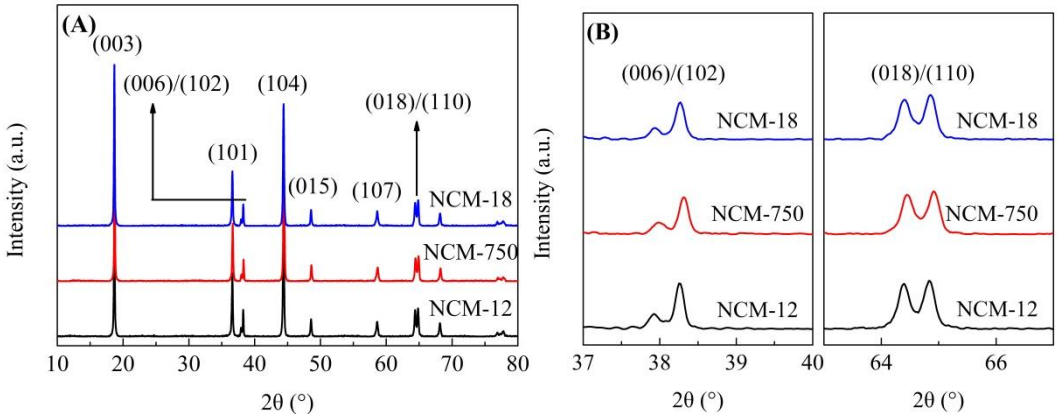

Figure 4. XRD patterns of NCM811 powders prepared at 750 °C for different sintering times.

3.2.2 Electrochemical Performances

Figure 5 (A) reveals the initial charge/discharge curves of different NCM materials between 2.7-4.3 V at 0.1 C. The discharge capacity of NCM-12 and NCM-18 is 167.7 and 192.6 mAh/g, which is evidently lower than that of NCM-750 (230.8 mAh/g). Subsequently, cycling performance of NCM811 active powders, which had undergone different sintering times, were carried out at 1 C by the galvanostatic system and the collected data are shown in Figure 5 (B). The cell coins assembled by the powder treated for 15 h (NCM-750) show excellent abilities both in the first discharge-capacity and capacity retention rate. These excellent performances can be mainly attributed to the best ordered-layered structure, as shown in Figure 4. It is noteworthy that the 100th discharge capacity of NCM-750 (140.4 mAh/g) is even higher than the 1st discharge capacity of NCM-12 (120.7 mAh/g) and NCM-18 (130.4 mAh/g). In addition, Figure 5 (C) displays the rate capability of the prepared active materials tested at 0.1~5 C. Similarly, the rate capability of NCM-750 (108.3 mAh/g) is dominantly higher than that of NCM-12 (64.12 mAh/g) and NCM-18 (40.68 mAh/g) especially when tested at a high rate of 5 C.

In order to further comprehend the influence of sintering time on the electrochemical properties of NCM811, EIS was adhibited to measure the resistances of various samples. The initial R_{ct} of NCM-12 (527 Ω) and NCM-18 (598 Ω) are superiorly higher than NCM-750 (179.9 Ω) resulting in poor first discharge capacity. Likewise, the large R_{ct} of NCM-12 (980.4 Ω) and NCM-18 (1226 Ω) compared with that of NCM-750 (404.2 Ω) leads to a rapid capacity fading of the cathode materials. As a result,

NCM811 displays an excellent electrochemical performance when sintered for 15 hours owing to the low R_{ct} which means Li^+ is able to move rapidly during intercalation/deintercalation [38-39]. Wang has reported that with the decrease of R_{ct}, D_{Li^+} increased from 1.15×10^{-12} to 1.14×10^{-11} cm^2/S, resulting in an improvement of electrochemical properties [39].

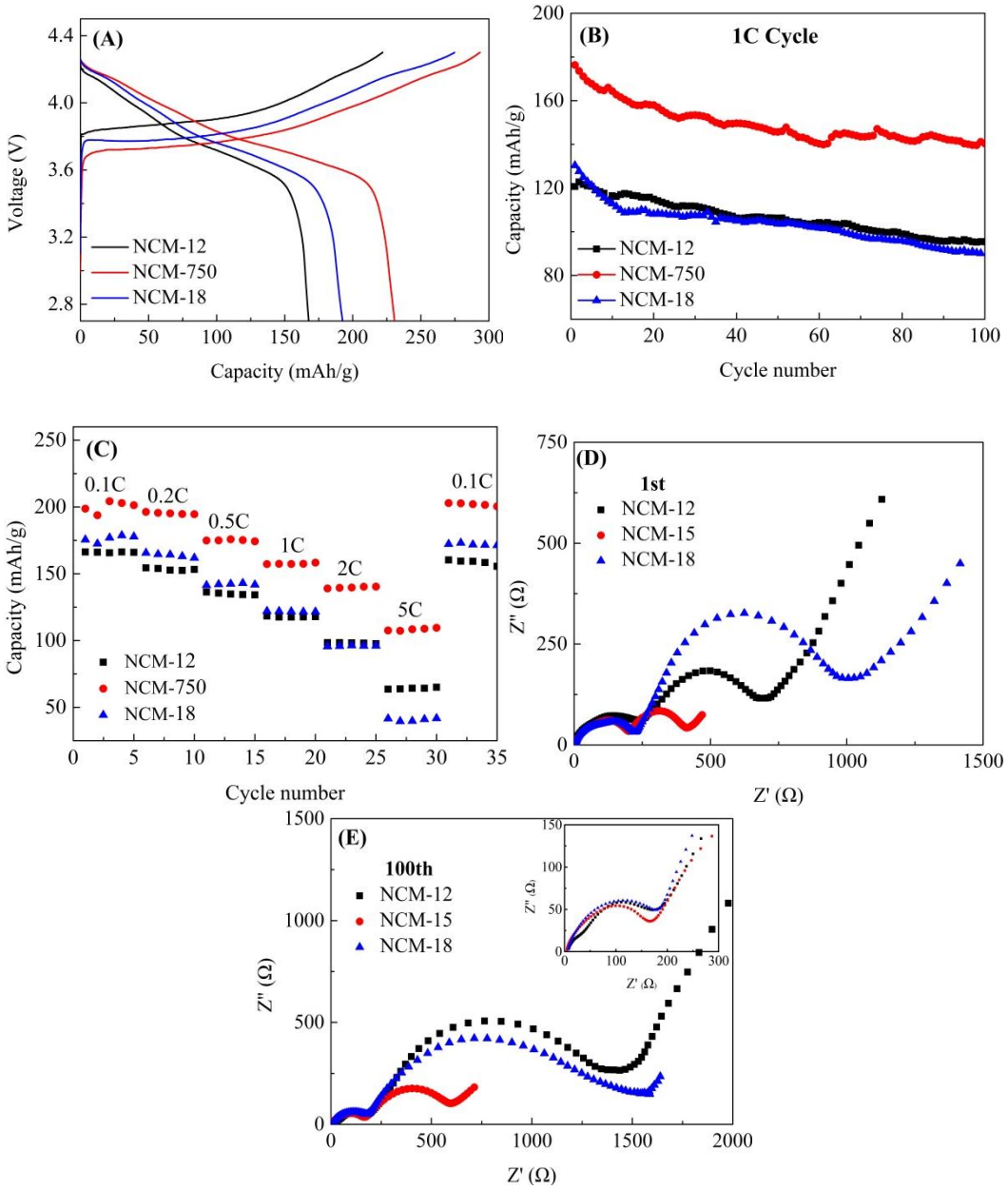

Figure 5. Electrochemical properties of NCM811 cathode materials prepared at 750 °C for different sintering times. (A) Initial charge/discharge properties at 0.1C, (B) Cycling performance at 1C, (C) Rate capabilities, (D) EIS curves for the initial cycle, (E) EIS curves after 100 cycling.

Therefore, the as-prepared NCM811 exhibits optimum performances when sintered at 750 °C for 15 hours, which is mainly attributed to the well-developed crystalline structure and appropriate morphology. The electrochemical properties of Ni-rich NCM cathode materials which synthesized by sol-gel method were listed in Table 4 for comparison. It can be concluded that NCM811 synthesized at

suitable sintering sonditions shows superior initial discharge capacity at 0.1 C as well as the highest discharge capacity at 1 C. In addition, a capacity retention rate of 79.6% after 100 cycling can also be obtained.

Table 3. Fitted parameters obtained from EIS shown in Figure 5 (D) and (E).

Sample	At the 1st cycle			At the 100th cycle		
	$R_s(\Omega)$	$R_{sf}(\Omega)$	$R_{ct}(\Omega)$	$R_s(\Omega)$	$R_{sf}(\Omega)$	$R_{ct}(\Omega)$
NCM-12	3.019	192.8	527	2.941	230.1	980.4
NCM-750	1.901	206.6	179.9	2.665	173.5	404.2
NCM-18	0.340	211.8	598	5.584	172.6	1226

Table 4. Electrochemical properties of NCM cathode materials synthesized by sol-gel method.

Cathode materials	Initial capacity at 0.1 C (mAh/g)	Initial capacity at 1 C (mAh/g)	Capacity retention rate at 1 C	Ref.
NCM811	199.9	-	82.5% (50^{th})	[16]
NCM811	200	162	75.8% (100^{th})	[17]
NCM811	182	161	81.61% (50^{th})	[18]
NCM622	174	143	87% (100^{th})	[19]
NCM622	196.07	-	65.2% (200^{th})	[40]
NCM811	230.8	176.3	79.6% (100^{th})	This work

4. CONCLUSION

Ni-rich layered cathode material NCM811 was successfully synthesized through a two-step sol-gel method by sintering the starting materials at different temperatures and times. The results illustrated that pure NCM811 must be synthesized above 700 °C, and the sintering time (12-18 h) shows little influence on the phase structure. On the other hand, the particles grew larger with increasing sintering temperature, while the sintering time has little influence on the morphology. The sample sintered at 750 °C for 15 h displays the most well-developed layered structure and uniformly distributed grain sizes. Further, the initial discharge capacity of this sample reaches 230.8, 176.3, and 108.3 mAh/g at 0.1, 1 and 5 C, respectively. After 100 cycles at 1 C, more than 79% of the capacity was retained.

ACKNOWLEDGEMENTS
This work was supported by the National Natural Science Foundation of China (No. 61701369 and 61974114); the Natural Science Basic Research Plan in Shaanxi Province of China (No. 2018JM6070 and 2018JM5060). The authors would like to thank Ms Xiaoyan Wei (Laboratory of Xi'an Center of China Geological Survey) for SEM analysis.

References

1. A. Manthiram, B.H. Song and W.D. Li, *Energy Storage Mater.,* 6 (2017) 125-139.

2. F.T. Yu, Z.Q. Yuan, T. Yang and B. Qian, Phys. *Chem. Chem. Phys.,* 20 (2018) 19195-19207.
3. H.M.K. Sari and X.F. Li, *Adv. Energy Mater.,* 9 (2019) 1901597.
4. J. Yang and Y.Y. Xia, *ACS Appl. Materi. Inter.,* 8 (2016) 1297-1308.
5. J. Kim, H. Lee, H. Cha, M. Yoon, M. Park and J. Cho, *Adv. Energy Mater.,* 8 (2018) 1702028.
6. X.B. Lu, X.H. Li, Z.X. Wang, H.J. Guo, G.C. Yan and X. Yin, *App. Surf. Sci.,* 297 (2014) 182-187.
7. A.O. Kondrakov, H. Geßwein, K. Galdina, L.B.V. Meded, E.O. Filatova, G. Schumacher, W. Wenzel, P. Hartmann, T. Brezesinski, and J. Janek, *J. Phys. Chem. C,* 121 (2017) 24381-24388.
8. L.J. Li, X.H. Li, Z.X. Wang, H.J. Guo, P. Yue, W. Chen and L.Wu, *Powder Technol.,* 206 (2011) 353-357.
9. X.B. Zheng, X.H. Li, B. Zhang, Z.X. Wang, H.J. Guo, Z.J. Huang, G.C.Yan, D. Wang and Y.Xu, *Ceram. Int.,* 42 (2016) 644-649.
10. D. Vu and J. Lee, *Korean J. Chem. Eng.* 33 (2016) 514-526.
11. H.H. Sun, W. Choi, J.K. Lee, I.H. Oh and H.G. Jung, *J. Power Sources,* 275 (2015) 877-883.
12. Z.W. Xiao, Y.J. Zhang and Y.F. Wang, *T. Nonferr. Metal. Soc.,* 25 (2015) 1568-1574.
13. H.R. Mao, Y.J. Zhang, P. Dong , Z.Z. Shi , H.X. Liang, J.M. Liu, *Int. J. Electrochem. Sci.*,11 (2016) 10536-10545.
14. M. Dahbi, J.M. Wikberg, I. Saadoune, T. Gustafsson, P. Svedlindh and K. Edström, *J. Appl. Phys.*,111 (2012) 023904.
15. W. Ahn, S.N. Lim, K.N. Jung, S.H. Yeon, K.B. Kim, H.S. Song and K.H. Shin, *J. Alloy. Compd.,* 609 (2014) 143-149.
16. J.X. Wu, X.H. Tan, J.T. Zhang, L.M. Guo, Y. Jiang, S.N. Liu, T.Q. Zhao, Y.L. Liu, J.C. Ren, H.F. Wang, X.H. Kang and W.G. Chu, *Energy Technol.,* 7 (2019) 209-215.
17. H.Q. Lu, H.T. Zhou, A.M. Svensson, A. Fossdal, E. Sheridan, S.G. Lu and F.V. Bruer, *Solid State Ionics,* 249 (2013) 105-111.
18. M.T. Tung and V.D. Luong, *Vietnam J. Chem.*,54 (2016) 724-729.
19. S.W. Lee, H. Kim, M.S. Kim, H.C. Youn, K. Kang, B.W. Cho, K.C. Roh and K.B. Kim, *J. Power Sources,*315 (2016) 261-268.
20. H.L. Jia, W.C. Zhu, Z.H. Xu, X.X. Nie, T.T. Liu, L.J. Gao and J.Q. Zhao, *Electrochim. Acta,* 266 (2018) 7-16.
21. T. Li, X.H. Li, Z.X. Wang and H.J. Guo, *J. Power Sources,* 342 (2017) 495-503.
22. Y. Li, X.H. Li, Z.X. Wang, H.J. Guo and J.X. Wang, *J. Nat. Gas.Chem.,* 27 (2018) 447-450.
23. L. Wang, B. Wu, D.B. Mu, X.J. Liu, Y.Y. Peng, H.L. Xu, Q. Liu, L. Gai and F. Wu, *J. Alloy. Compd.,* 674 (2016) 360-367.
24. K.K. Cheralathana, N.Y. Kanga, H.S. Parka, Y.J. Leea, W.C. Choia, Y.S. Kob and Y.K. Park, *J. Power Sources,*195 (2010) 1486-1494.
25. Y. Liu, W.L. Yao, C. Lei, Q. Zhang, S.W. Zhong, and Z.Q.Yan, *J. Electrochem. Soc.,* 166 (2019) A1300-A1309.
26. Y.K. Xi, Y. Liu, D.K. Zhang, S.L. Jin, R. Zhang and M.L. Jin, *Solid State Ionics,*327 (2018) 27-31.
27. Y.F. Xia, M. Nie, Z.B. Wang, F.D. Yu, Y. Zhang, L.L. Zheng, J. Wu and K. Ke, *Ceram. Int.,* 41 (2015) 11815-11823.
28. M.L. Zhang, J.T. Shen, J. Li, D.Y. Zhang, Y.X. Yan, Y.X. Huang and Z.M. Li, *Ceram. Int.,* In Press.
29. J.M. Zheng, P.F. Yan, L. Esteveza, C.M. Wang and J.G. Zhang, *Nano Energy,* 49 (2018) 538-548.
30. D. Wang, X.H. Li, Z.X. Wang, H.J. Guo, Y. Xu, Y.L. Fan and J.J. Ru, *Electrochim. Acta,* 188 (2016) 48-56.
31. G. Yang, X.Z. Qin, B. Wang, F.P. Cai and J. Gao, J. Mater Sci, https://doi.org/10.1557/jmr.2019.307.
32. W.B. Hua, J.B. Zhang, Z. Zheng, W.Y. Liu, X.H. Peng, X.D. Guo, B.H. Zhong, Y.J. Wang and X.L. Wang, *Dalton Trans.,* 43 (2014) 14824-14832.
33. M. Wang, R. Zhang, Y.Q. Gong, Y.F. Su, D.B. Xiang, L. Chen, Y.B. Chen, M. Luo and M. Chu, *Solid State Ionics,* 312 (2017) 53-60.

34. T.X. Lei, Y.J. Lia, Q.Y. Su, G.L. Cao, W. Li, Y.X. Chen, L.L. Xue and S.Y. Deng, *Ceram. Int.*, 44 (2018) 8809-8817.
35. Q.L. Fan, S.D. Yang, J. Liu, H.D. Liu, K.J. Lin, R. Liu, C.Y. Hong, L.Y. Liu, Y. Chen, K. An, Ping Liu, Z.C. Shi and Y. Yang, *J. Power Sources*, 421 (2019) 91-99.
36. Y.C. Li, W. Xiang, Z.G. Wu, C.L. Xu, Y.D. Xu, Y. Xiao, Z.G. Yang, C.J. Wu, G.P. Lv and X.D. Guo, *Electrochim. Acta*, 291 (2018) 84-94.
37. D.L. Vu and J.W. Lee, J. *Solid State Electr.*, 22 (2018) 1165-1173.
38. X. Li, K.J. Zhang, M.S. Wang, Y. Liu, M.Z. Qu, W.G. Zhao and J.M. Zheng, *Sustain. Energ. Fuels*, 2018 (2) 413-421.
39. D. Wang, X.H. Li, Z.X. Wang, H.J. Guo, Y. Xu, Y.L. Fan and J.J. Ru, *Electrochim. Acta*,188 (2016) 48-56.
40. Y.Q. Wu, M.L. Li, W.D. Wahyudi, G. Sheng, X.H. Miao, T. D. Anthopoulos, K.W. Huang, Y.X. Li, and Z.P. Lai, *ACS Omega*, 4 (2019) 13972-13980.